The deformation-DIA: A new apparatus for high temperature triaxial deformation to pressures up to 15 GPa

Yanbin Wang[a)]
GeoSoilEnviroCARS, The University of Chicago, 5640 South Ellis Avenue, Chicago, Illinois 60637

William B. Durham
Lawrence Livermore National Laboratory, P.O. Box 808, L-201, Livermore, California 94550

Ivan C. Getting
CIRES, University of Colorado, Boulder, Colorado 80309

Donald J. Weidner
Department of Earth and Space Science, State University of New York at Stony Brook, Stony Brook, New York 11794

(Received 5 November 2002; accepted 25 February 2003)

A new deformation apparatus has been developed, based on the widely used cubic-anvil apparatus known as the DIA. Two differential rams, introduced in the upper and lower guide blocks, allow independent control of the differential strain and stress field under high confining pressure. Testing experiments with synchrotron x rays have demonstrated that this deformation DIA (D-DIA) is capable of generating up to 30% axial strain on a 1–2 mm long sample under confining pressures up to 15 GPa at simultaneous high temperatures. Various compressional strain rates from 10^{-3} to about 5×10^{-6} s^{-1} have been achieved. Extensional experiments have also been carried out successfully. Strains are measured by x-ray imaging of the sample which has a length measurement precision of $\sim$0.1 μm; pressures are monitored using standard materials with well established equations of state. X-ray transparent anvils made of sintered polycrystalline cubic boron nitride have been successfully tested, with a two-dimensional x-ray charge coupled device detector. Distortions in the diffraction lines due to differential stress can be measured with a precision of about 20 MPa.
 [DOI: 10.1063/1.1570948]

I. INTRODUCTION

Quantitative studies of rheological properties of materials under high pressure have been limited due to technical difficulties with containing pressure and with accurately measuring stress. For example, in earth sciences, quantitative experimental studies of rheological properties of rocks and minerals as well as deformation-induced microstructures have been mostly limited to conditions below 4 GPa. The best-resolved measurements of stress and strain rate are made in a gas pressure vessel, whose design limits are usually 0.3–0.5 GPa, corresponding to a depth of 10–15 km in the earth, and rarely exceed 1 GPa.[1] Less accurate measurements are possible to 4 GPa in solid-medium devices such as the Griggs apparatus. With modifications to apparatus size, sample assembly, and institution of a molten salt confining medium, a Griggs apparatus can be used for quantitative rheological studies,[2] but the maximum pressure of its operation is still about 4 GPa,[3,4] corresponding to a depth of about 120 km. As a consequence, rheological properties of more than 90% of Earth's mantle remain unexplored in a quantitative manner.

As another example of the need for rheological experiments at very high pressures is the need of better understanding of materials and processes of nuclear weapons in the absence of nuclear testing[5] far beyond levels reached to date. Work hardening of certain body-centered-cubic metals, for example, shows a pronounced dependence on pressure up to 3 GPa,[6] but has never been explored under controlled conditions at higher pressures.

Many techniques have been developed to address this need. Kinsland and Bassett[7] and Sung *et al.*[8] used the diamond-anvil cell (DAC) as a deformation apparatus. In their technique, a sample was sandwiched between two single crystals of diamond and radial distribution of pressure was determined by measuring the shift of fluorescence lines of ruby crystals located at various points in the sample chamber. Assuming that the pressure gradient was supported by the sample strength, one could then estimate the sample's strength based on the equation of force balance. Such a technique has been used extensively at room temperature to the pressure of $\sim$40 GPa.[9–12] The major advantage of this technique is the high pressures that can be achieved. However, there are major limitations with this approach: (1) homogeneous heating is difficult in the DAC, and almost all previous results were obtained at room temperature; (2) the rate of deformation is not well constrained and deformation is likely to be time dependent in these tests; (3) the sample chamber is extremely small (typically microns to tens of microns) so that some important effects such as grain-size sensitivity of

a)Author to whom correspondence should be addressed; electronic mail: wang@cars.uchicago.edu

strength are difficult to measure; and (4) pressure generation and deformation are coupled.

There have been many efforts in using the multianvil press as a deformation machine. In the multianvil press, pressurization is approximately hydrostatic, and compression of a sample is normally isotropic. However, by making the mechanical strength and elastic stiffness of a sample assembly anisotropic, one can create a deviatoric stress field in the sample assembly. This deviatoric stress is relaxed by plastic flow upon heating. This technique has been used in a number of studies.[13–19] Analyses[17,18] showed that the mode of deformation in this technique is in most cases ''stress relaxation,'' i.e., the magnitude of deviatoric stress changes significantly within a single experiment. The amount of piston movement in this technique is limited and hence the strain magnitude is limited. However, by using a thin sample sandwiched between two pistons cut at 45° to the strong/stiff direction, Karato and Rubie[17] were able to attain relatively large strains ($\sim$1–2).

Quasiconstant displacement rate tests can also be made with the multianvil press through continuous movement of the ram.[15,16] Nevertheless, the maximum amount of strain attained by this mode of operation is limited because the confining pressure also changes with deformation and gasket extrusion eventually stops. The multianvil deformation technique has been applied to $\sim$25 GPa and $\sim$2000 K with a sample dimension of $\sim$1–2 mm diameter and $\sim$2–4 mm long, or a thin ($\sim$0.2 mm) disk sample with a similar diameter.[20] The major advantage of this technique as compared to the DAC technique is that rheological properties can be investigated under more homogeneous high temperature and pressure conditions with better-controlled chemical environment. Also, because relatively large samples can be used, microstructural evolution during deformation and its effects on rheology can be investigated.[19] This technique has two major limitations, however. First, as in the DAC, pressurization and plastic deformation cannot be completely separated and deformation during pressurization likely occurs unless special care is taken in the sample assembly to absorb initial stage shape change of sample assembly.[17,18] Second, because the stress magnitude changes during an experiment, dominant mechanisms of deformation may change in a single run, making interpretation of mechanical data and microstructure difficult.

Yamazaki and Karato[21] modified the Drickamer-type high-pressure apparatus to achieve high strain. One of the anvils is fixed with the frame, whereas the other is attached to a rotational actuator. The sample is twisted between the two pistons, and the geometry of deformation is rotational shear (i.e., simple shear in any radial plane). Yamazaki and Karato reported that with their motor and gear combination, shear strain rates from $\sim$0 to $\sim 10^{-3}$ s^{-1} can be achieved. Extremely large strains (in principle unlimited) can be attained. However, it is difficult to quantify the stress–strain relationship.

To achieve controlled deformation under high pressures, Carter *et al.*[22] and later Shimada[23] deployed a cubic press, which drives six independent hydraulic rams to push six square-tipped anvils, compressing a cubic pressure medium.

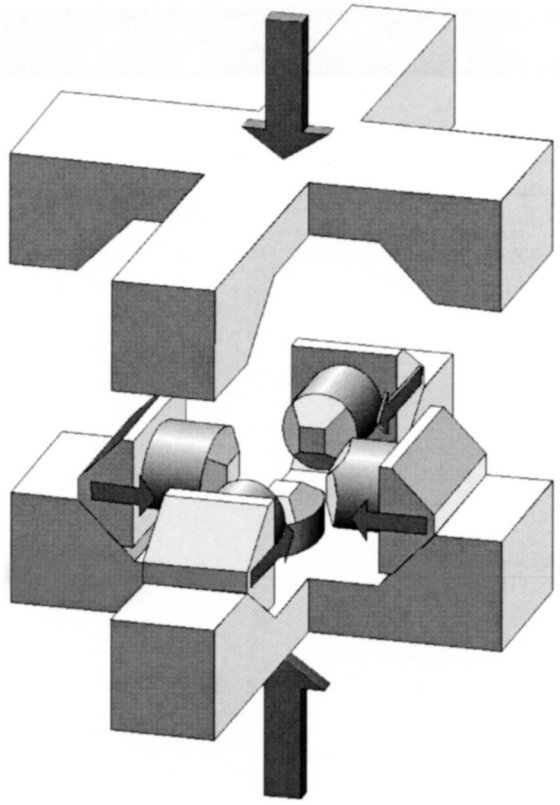

FIG. 1. Conceptual diagram illustrating the principles of the DIA cubic anvil apparatus.

To perform triaxial deformation tests, the upper and lower anvils are advanced independently while keeping the four horizontal anvils fixed. However, precise manipulation of six independent hydraulic rams is both expensive and operationally complicated. No new activities were reported after initial deployment of this apparatus.

In this article, we report a new high-pressure deformation apparatus that is capable of generating pressures up to 15 GPa (or about 450 km depth in the earth) at high temperatures (up to $\sim$2000 °C). This apparatus is a modification of the cubic-anvil apparatus known as the DIA,[24,25] which is widely used in solid-media hydrostatic compression experiments coupled with synchrotron x-ray diffraction.[25–28] This apparatus takes advantage of recent developments using synchrotron radiation to allow measurement of displacement and stress to resolutions of <1 μm and $\sim$20 MPa, respectively, thus making it possible to perform quantitative deformation experiments under pressure and temperature conditions reaching the Earth's transition zone.

II. DESIGN CRITERIA

A. Overview of configuration

The original DIA consists of symmetric upper and lower guide blocks, four wedge-shaped thrust blocks (''side wedges''), and six anvils, as indicated in Fig. 1. Four of the anvils are mounted on the inside faces of the side wedges and the other two are mounted on the inside central faces of the guide blocks, the square, truncated fronts of the anvils thus defining a cubic volume at the center of the apparatus.

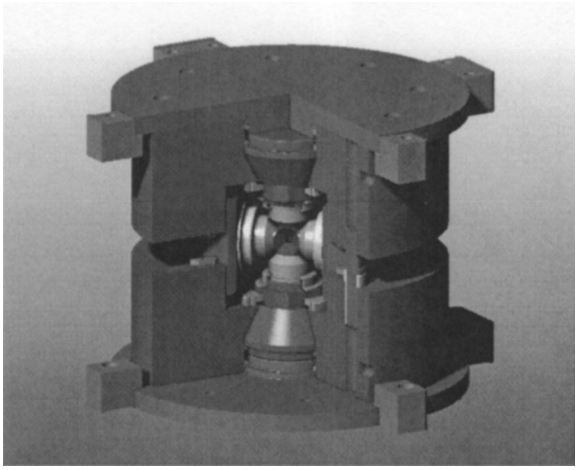

FIG. 2. Cutaway view of the D-DIA with differential rams in the upper and lower guide blocks. Note locations of the differential rams.

The operation of the DIA can be visualized by recognizing that the eight inner inclined surfaces of the guide blocks define a virtual regular octahedron whose dimension changes with the separation distance between the guide blocks. The six anvils are aligned with the six apices of this virtual octahedron, and parts are machined such that the (fixed) distance from anvil face to associated apex of the virtual octahedron is precisely the same for each anvil. As the guide blocks close or open, all displacements of the anvils are therefore symmetric about the center. The force of a single hydraulic actuator (or ram) applied along the vertical axis in Fig. 1 closes the guide blocks and thus compresses the cubic sample/furnace assembly hydrostatically.

In our new apparatus, called the deformation-DIA (or D-DIA), independent control of the displacement of one anvil pair is provided by two additional hydraulic actuators, called differential rams. The differential rams are located within the guide blocks of the D-DIA module (Fig. 2) and react against the platens driven by the main hydraulic ram, which provides the hydrostatic pressurization. Note that in the D-DIA modification, the guide blocks not only support the forces confining the side wedges, they now have also become thick-wall pressure containers for the hydraulic fluid driving the differential rams. For this reason, the guide blocks of the D-DIA are complete disks rather than crossed steel members as in the original DIA (Fig. 1).

The unique capability of independent control of the differential rams now allows deformation to be imposed without simultaneously increasing confining pressure (which has been the long-standing limitation of multianvil devices and the DAC as deformation machines). In normal operation, the D-DIA sample is brought to run conditions of P and T with differential rams fully withdrawn in the same manner as the hydrostatic DIA. Advancing the differential rams then introduces a noncubic shape change to the assembly. At the same time, by simultaneously draining hydraulic fluid from the main ram at an appropriate rate, the four side anvils retract, and the total force of the main ram as well as the volume of the sample cell are held constant. In the synchrotron x-ray beamline (more below) pressure itself can be monitored and so serves as the process variable.

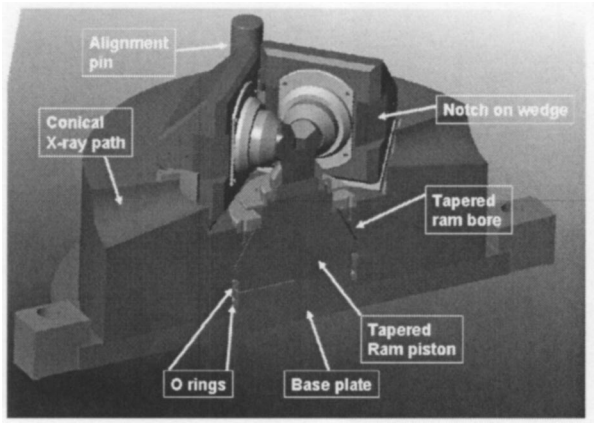

FIG. 3. Details of the differential ram design and modification in the wedges for wider x-ray access.

B. Load consideration

Typical main ram forces are up to ~100 T in the hydrostatic DIA. Maximum attainable pressures vary depending on the anvil truncation size. When tungsten carbide (WC) anvils are used, the maximum pressures are about 7 GPa for 6 mm truncation anvils (sample cell length 8 mm), 10 GPa for 4 mm (6 mm cell), and 13 GPa for 3 mm (5 mm cell), respectively.[29,30] Wang *et al.*[31] showed that with a slight taper (4°) near the anvil tip, the modified 4 mm anvils can reach pressures about 35% higher than the nontapered anvils. With sintered diamond and possibly with cubic boron nitride anvils, pressures up to 18 GPa are achievable with 3 mm truncation.[30]

Ignoring friction between all the sliding surfaces and any shear strength in the cell assembly, the thrust on each anvil is 1/3 of the main ram force. The maximum main ram load is 100 T, thus in hydrostatic compression (without applying differential load) each anvil will support up to 33.3 T load. In order to generate sufficient differential strain in the sample, the differential rams are designed to be capable of twice that load (62 T). Such load capacity is sufficient to overcome the confining force and to apply differential force even at the highest confining pressure. This is achieved with a differential ram diameter of 89 mm and maximum allowable working pressure of 100 MPa.

C. Differential rams

Typical sample dimensions are 1 mm diameter and 1–2 mm in length. Each differential ram has a travel of 2 mm, which, accounting for some of the displacement partitioned to elasticity and to other cell parts, is sufficient to provide shortening (engineering) strains of 50% or more in the sample.

The differential rams have a piston that has a tapered cross section (Fig. 3). A backing plate is used to seal the oil chamber and a small hole through the wall of each guide block allows input of hydraulic fluid to each ram. Both the piston and the backing plate have a ledge for the O-ring assembly. Sealing is achieved by Parker (N0552-90) O-rings (Nitrile, 90 durometer A), with Parker Parbak N0300-90 backup rings.

The differential rams are driven by high-precision positive-displacement pumps, and their velocities are controllable from approximately 10^{-7} to 10^{-2} mm/s. When both rams are driven symmetrically, this translates to a strain rate on a typical 1 mm length, 1 mm^3 volume sample of approximately 10^{-2}–10^{-7} s^{-1}, again accounting for some displacement partitioned to other parts of the load column. These rates are much faster than most relevant rates in geology, but as with all experimental rock mechanics work—for which these rates are typical—it is the human time scale and not the geologic time scale that governs the duration of an experiment. As with most experimental studies of rock deformation, appropriate scaling analysis is critical to apply these results to Earth. Differential ram displacements of >1 mm are possible, so strains in pure shear compression can approach 1. Deformation in simple shear, using 45°-cut pistons is also possible, allowing for much higher strains, at some cost to sample volume. Finally, the D-DIA is capable of extensional, as well compressional deformation, since the sense of motion of the six anvils can be reversed.

D. X-ray access

A crucial requirement for the D-DIA is the ability to perform diffraction and imaging analyses on the sample using synchrotron x radiation. The original hydrostatic DIA has been widely used for synchrotron applications.[25,27,28] However, in the past, diffraction has been limited to near the vertical plane only. This is largely due to the anvil material of choice, namely WC, which is highly attenuating to x rays. In order to allow precise measurement of both hydrostatic pressure and deviatoric stress using x rays, multiple diffractions at various angles in the plane perpendicular to the incident x rays must be observed.[32,33] To facilitate this, conical openings are made into the guide blocks, so that a $\pm 10°$ solid angle can be accessed (Fig. 3). Notches are made in the anvil-supporting side wedges to give access to the entire $\pm 10°$ solid angle. With the advent of new anvil materials such as sintered diamond or cubic boron nitride (cBN), this configuration allows us to measure diffraction at any orientation.

III. FINITE ELEMENT ANALYSES

Three-dimensional finite element analysis (FEA) of the D-DIA guideblocks shows that the maximum octahedral stress occurs on the inner bore in an operation where the differential load is at its maximum load capacity, i.e., 62% of the maximum main ram load. The stress at the base of the inclined surface of the guideblock, the next highest point of stress concentration in the guide block, is roughly 90% of the stress in the bore. Note that in the original DIA with very large notches cut in the guide blocks, the stress concentration at the base of the inclined surfaces is twice that of the D-DIA under similar main ram load.

Two-dimensional, axisymmetric FEA was carried out on the differential ram itself for a differential ram hydraulic pressure of 105 MPa. Figure 4(a) shows Von Mises stress magnitude in the differential ram piston. The piston is a combination of a cylinder and a cone. Rotating the cross section

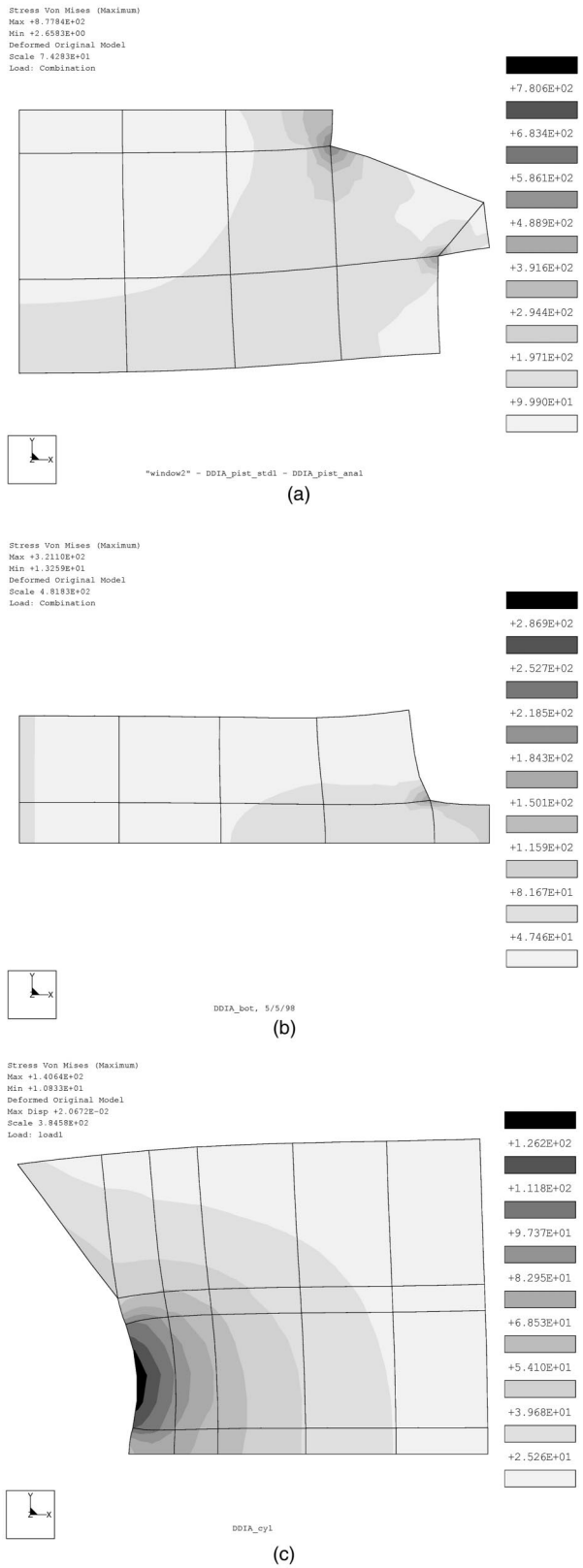

FIG. 4. (a) Von Mises stress and deformation of the differential ram piston. (b) Von Mises stress magnitude in the ram base plate. Maximum stress occurs at the lower right corner, in the order of 120 MPa. Maximum displacement is 7 μm, which occurs near the upper right corner. (c) Displacement and Von Mises stress in the guide block, which is approximated as axial symmetric. Maximum Von Mises occurs on the inner wall of the ram, around 140 MPa. Maximum displacement about 20 μm occurs at the same location, almost pure radial.

in Fig. 4(a) by 360° will complete the shape. The maximum stress (877 MPa) that occurs at the sharp corners in the piston is clearly an artifact. In reality, the corners are rounded with a 2 mm radius, which should greatly reduce the stress concentration. Away from the corners, the highest Von Mises stress is in the 300 MPa level.

Figure 4(a) also shows exaggerated displacement field. The maximum displacement occurs in the lower right corner and is 40 μm and almost purely vertical.

Similar FEA results on the ram base plate and the guide block are summarized in Figs. 4(b) and 4(c). For the ram base plate, maximum Von Mises stress is on the order of 120 MPa if the corner effect is removed and maximum displacement is only 7 μm in the upper right corner.

IV. MECHANICAL SETUP

A. Guide blocks

Figure 5(a) shows the actual D-DIA guide blocks, which are mounted in a die set to allow easy transport in and out of the hydraulic press used for pressure generation. The die set has four ball-bearing rollers to allow the entire unit to be rolled in and out of the press on rails. A vertical displacement transducer [a linear variable differential transformer (LVDT)] is used to monitor closure between the top and bottom guide blocks during the experiment, and a horizontal LVDT is mounted to the back of one of the four side wedges to monitor the travel of the horizontal anvils during deformation. Four miniaturized displacement transducers [differential variable reluctance transducers (DVRTs)] (MicroStrain, Inc., Burlington, VT) are used to measure differential ram displacements [Fig. 5(b)].

B. Hydraulic control

Hydrostatic pressure is generated to the same levels and in the same manner as with the hydrostatic DIA. To apply an additional deviatoric stress field, the upper and lower anvils are pushed simultaneously towards the center of the sample assembly. To maintain the tetragonal symmetry in the presence of frictional imbalances, the two differential rams are independently controlled such that they travel by the same amount. However, any increase (or decrease) in pressure in the differential rams will raise (or lower) the main ram pressure. Accordingly, fine control on the main ram is needed to drain (or supply) hydraulic fluid and maintain a constant pressure.

We use three positive displacement pumps (PDPs) to drive the three hydraulic systems. Each is driven by stepper motors and controlled by computer. Each of the two PDPs used to control differential ram displacement has a capacity of ~10 cc, or roughly one full stroke of each differential ram. The third has a capacity of ~30 cc and is connected in parallel to the hydraulic ram of the main press. The motor speed of the differential ram PDPs can be controlled to drive the differential rams at displacement rates ranging from arbitrarily slow to 0.01 mm/s. The motor speed of the main ram PDP is sufficient to react accordingly.

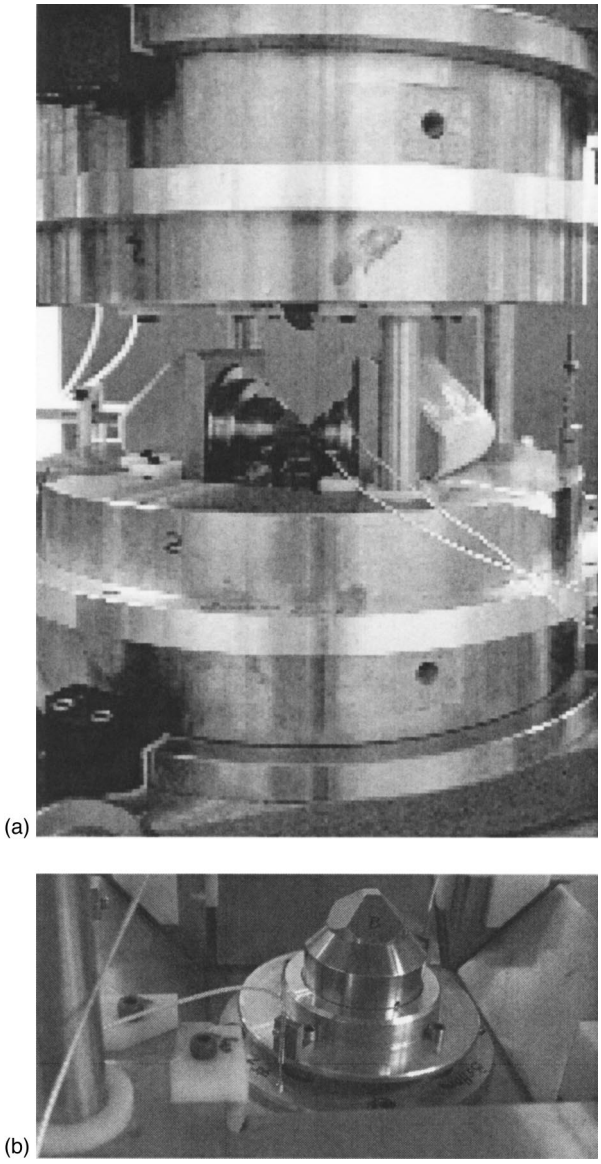

FIG. 5. Actual D-DIA tested: (A) overall view of the setup and (B) details of the DVRTs used for monitoring differential ram displacement during deformation.

V. TEST RESULTS USING SYNCHROTRON X-RAY SOURCES

To perform quantitative deformation experiments in the D-DIA, one needs to be able to measure both stress and strain under high pressure since conventional load cell and strain gage techniques cannot be used in a solid pressure medium apparatus such as the D-DIA. With the advent of synchrotron x-ray techniques, two well-established synchrotron x-ray detection techniques can be used for these purposes. The D-DIA can readily be fitted to synchrotron radiation facilities to allow quantitative measurements of stress and strain at high-pressure and temperature conditions.

Figure 6 shows a typical 6 mm cell assembly used for the tests. Both pyrophyllite and a boron–epoxy mixture are used as pressure media, with a thermocouple entering the cylindrical graphite heater (4 mm long) from the top. Temperature gradients at 1273 K, estimated from unit cell volume measurement on NaCl along the axial direction, were

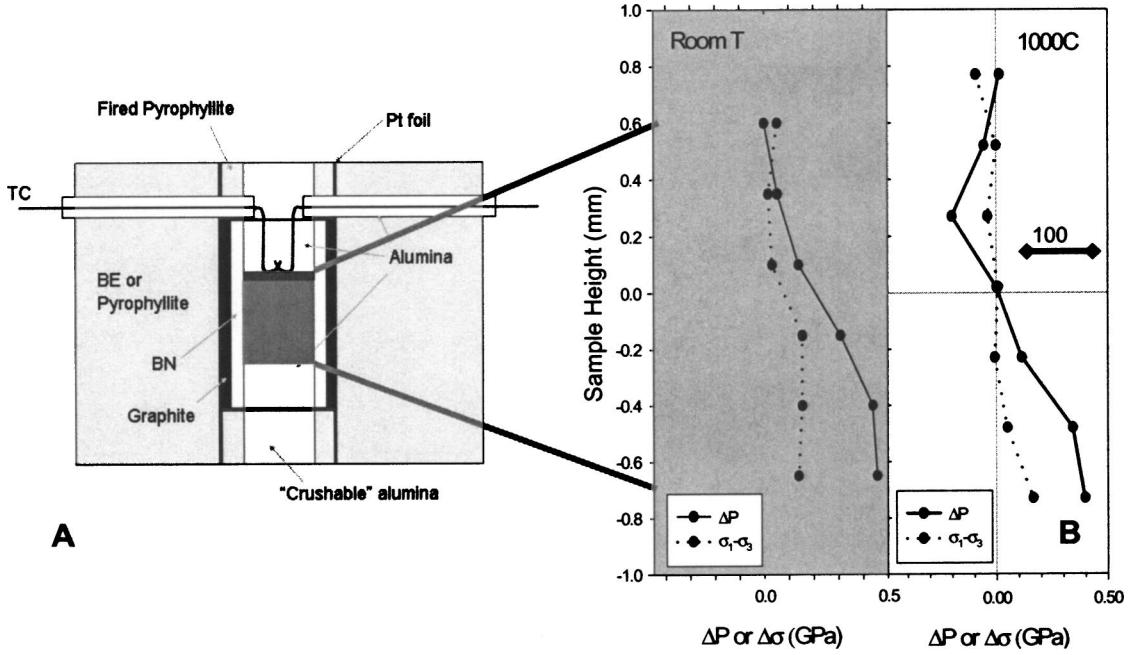

FIG. 6. (A) Cell assembly used in deformation experiments. Total sample length is typically 2 mm, located in the center of the graphite heater. (B) Measured pressure and temperature gradients throughout a 2 mm long NaCl sample at room temperature and 6 GPa (left) and 1000 t°C (right), without advancing the differential rams (i.e., quasihydrostatic compression). Dots with solid line are pressure difference with respect to the pressure (6 GPa) measured at top of the sample Note increase in apparent pressure from top to bottom at room temperature. The differential stress, calculated using relative peak shift in NaCl, reaches its yield strength (~0.2 GPa) throughout the bottom half of the sample. The increase in apparent pressure can be well explained by the differential stress (Ref. 27). At 1000 °C, strength of NaCl is negligible and all the observed pressure variation is attributable to temperature gradient. According to NaCl equation of state, the pressure variations correspond to about 100 °C temperature variations, most of which is near the bottom 0.2 mm of the sample.

about 100 K within the center 2.0–2.5 mm and within 50 K over a 1 mm length near the center. Crushable alumina (porosity about 30%) end plugs were used to minimize axial deformation during cold compression.

A. Sample length and strain measurement

We have successfully tested the D-DIA at both the National Synchrotron Light Source, using the SAM-85 system at beamline X-17B1,[27] and the Advanced Photon Source, using the 250 ton system in 13-BM-D at GSECARS.[28,34] Figure 7 is a computer screen print showing the vital information being monitored and controlled for the D-DIA during deformation of a fully densified polycrystalline Mo sample. We monitored the differential ram displacements (by the four DVRTs) as well as ram hydraulic pressures. During deformation both differential rams were advanced at a controlled rate of about 1.5×10^{-5} mm/s, resulting in a total cell shortening rate of 3×10^{-5} mm/s. The differential ram pressures (PT1 and PT2) steadily increased even though the displacement rate and pressure were steady, probably because gasket tractions around the differential ram anvils were steadily increasing. These gaskets are the result of extrusion of the pressure medium under increasing pressures; they serve as pressure seals and provide lateral support on the anvils through increasing normal stress on the anvil flanks. Note that because of the increasing differential ram force, some of the displacement registered by the DVRTs is elastic compression of the ram and anvil. The advance of the differential rams also caused the main ram pressure (PT3) to increase. In order to maintain a constant cell pressure, the main ram pressure was decreased. From this point on, the differential rams were at a more or less constant pressure.

Based on results to date, most of the ram force is distributed between supporting hydrostatic pressure and supporting normal and shear forces on the gaskets. Because of its relatively small cross-sectional area, the strength of the sample column contributes negligibly (at our current ability to resolve) to the ram force.

Both the vertical guide block gap and the horizontal anvil displacement were also monitored by LVDTs. The observations show that as the differential rams were advanced and main ram pressure reduced, the vertical guide block gap steadily increased, due to the extra force exerted by the differential rams. Also as the top and bottom anvils advanced, the horizontal anvils retracted. All these observations confirmed that the D-DIA was behaving as expected and capable of producing up to 1 mm shortening in the cell assembly.

Synchrotron x rays were also used to measure sample length. Direct images of markers were obtained using an incident beam typically 2×3 mm^2 in dimension and markers with contrasting absorption characteristics. Platinum or gold foils above and below the sample could be easily viewed. The image was obtained by projecting the x-ray intensity contrast through the cell onto a fluorescent screen that is viewed with a charge coupled device (CCD) camera though a magnifying system.[28] By analyzing the images during the deformation, sample length change and strain can be determined (see Fig. 8). Another potential technique is to detect fluorescence of the marker material used in the cell to define the ends of the sample.[35] In either case, it has been demon-

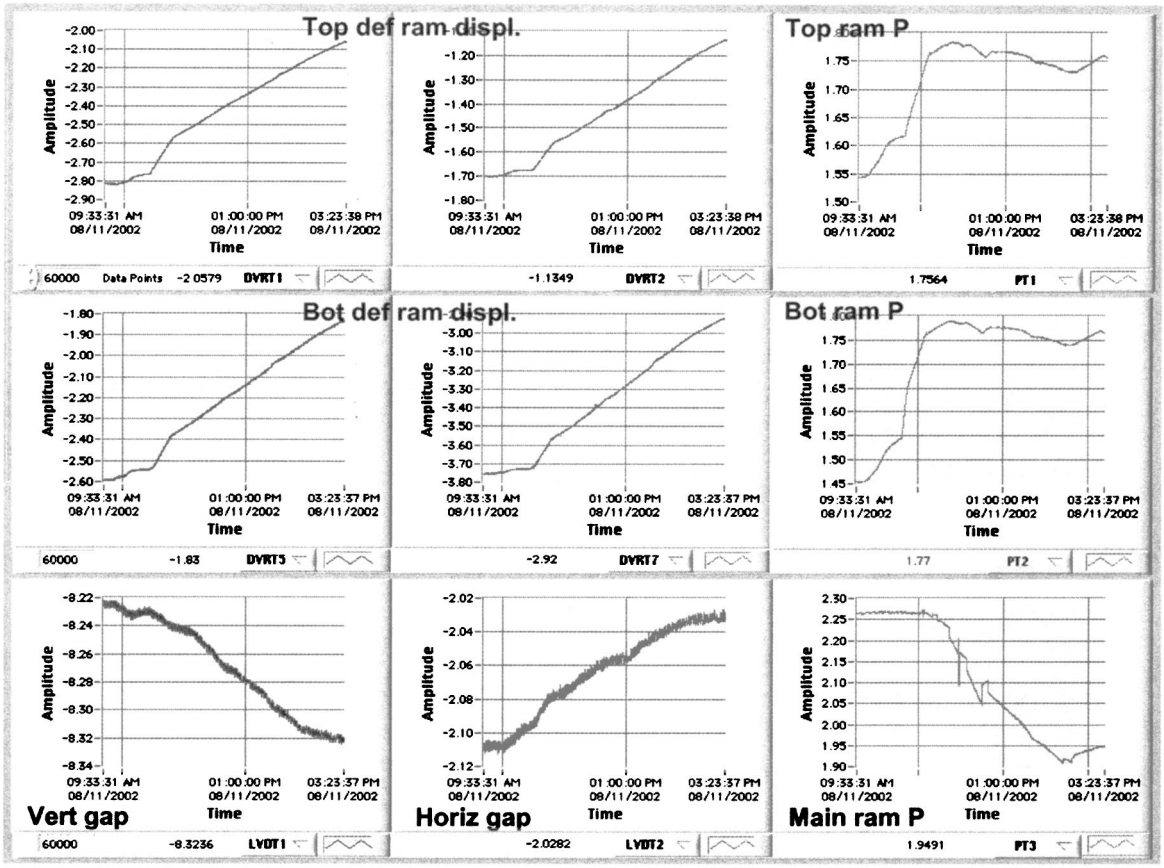

FIG. 7. Example of control record showing machine parameters during a deformation experiment (D0374). DVRT1 and 2 are the transducers monitoring displacement on the top differential ram; DVRT5 and 7 for the bottom differential ram. Amplitudes are in volts (1 V~0.5 mm). Pressures in the differential rams are monitored by the pressure transducers, PT1 and 2, with calibration constant 1 V~6000 psi. LVDT1 and 2 are for gap between guide blocks and horizontal anvil outward displacement, respectively (calibration constants: 1 V~−2.54 mm).

strated that a sample length can be measured to within 1 μm and sample length change to within 0.1 μm. With a sample length of 1–2 mm, this means that strains of 10^{-4} or better can be measured.

Figure 8 shows sample length as a function of time during an experiment where a fully densified polycrystalline Ta sample (1 mm long) was ''piggybacked'' with a sample of mixed Au and MgO at 8 GPa and 1273 K. Sample length change was measured from digital x-ray imaging. Within about 5 h, the sample was shortened axially by 0.2 mm (about 20%). In this particular cell assembly, 50% of the 0.4 mm total shortening (as indicated by the DVRT records) was transmitted to the sample.

X-ray imaging also confirmed the horizontal anvil displacement observations from the LVDT measurement. Figure 9 shows the measured anvil gap change during deformation of a Mo sample with MgO. The rate of gap opening is in the same order of magnitude as the sample shortening in this experiment.

In a separate experiment, two samples, polycrystalline rods of MgO and Ta were piggybacked in one cell assembly and deformed under a hydrostatic pressure of 10 GPa at 773 K. The pressure was measured by x-ray diffraction and based on the equation of state of MgO,[36] and sample lengths of MgO and Ta were determined using x-ray imaging. Figure 10 shows strains measured from the two samples under those conditions. Evidently Ta and MgO have similar flow properties. Pressure and temperature were both held constant during the deformation.

Various strain rates have been achieved, ranging from 10^{-4} to about 5×10^{-6} s^{-1}. We see no difficulties in reaching much slower strain rates to about 10^{-7} s^{-1}.

B. Stress measurement

The technique for measuring elastic strain using x-ray diffraction to obtain information on stress in materials dates back at least to the 1930s.[37–39] Applications to high pressures *in situ* have become feasible using high-energy x rays generated by a synchrotron source.[32,40] Knowledge of x-ray energy and diffraction angle (Bragg angle) is sufficient to determine the distance between lattice planes (called *d* spacing) of the crystalline sample. The *d* spacing is insensitive to plastic strain, reflecting only the elastic strain field. In a nonhydrostatic stress field, crystallographic planes at different orientations to the principal stress directions change their *d* spacing to a different degree. For polycrystalline samples where grains are randomly oriented, each spacing is seen as a continuous diffraction ring (called the Debye ring) that is circular if stress is purely hydrostatic and distorted if stress has a deviatoric component. By measuring the shape and size of the Debye ring, one determines the orientation depen-

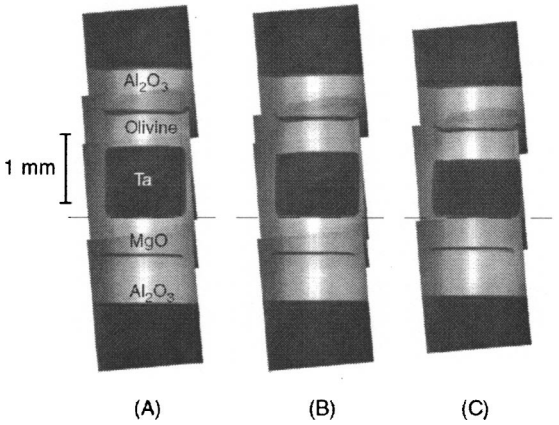

FIG. 8. Composite digital radiographs of a polycrystalline sample of Ta deformed at 8 GPa pressure (A) before deformation, (B) after 10% strain at room temperature at a rate of 4.5×10^{-5} s^{-1}, and (C) after an additional 10% strain at 1273 K and the same rate. X-ray diffraction intensity is strongly attenuated in the Ta, so pressure/stress indicators of olivine $(Mg_{0.9},Fe_{0.1})_2SiO_4$ and MgO surround the sample. Gold foils mark the interfaces between the cold, hard Al_2O_3 pistons and the olivine and MgO. Note that the olivine and MgO have also strained, especially at the higher temperature.

dence of a particular *d* spacing and therefore the total stress magnitude (hydrostatic plus deviatoric) using the known elastic moduli of the crystal. As discussed above, the anvils themselves cast a shadow and limit the region where the diffracted signal can be observed. However, with the development of new anvil materials, especially cBN, which is x-ray transparent, it is now possible to observe the entire Debye ring.

We have measured distortion of the Debye rings in the D-DIA with cBN anvils and monochromatic diffraction using a Bruker SMART1500 x-ray CCD detector. Figure 11 compares monochromatic diffraction patterns of MgO recorded at both ambient condition and at about 9 GPa and

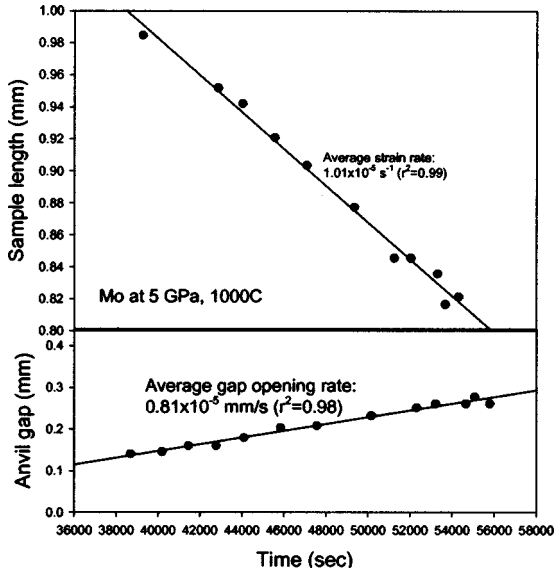

FIG. 9. Deformation of a polycrystalline Mo sample (1 mm) at 5 GPa and 1000 °C. Upper panel shows sample length measurement, which gives a strain rate of 10^{-5} s^{-1}. Lower panel shows associated horizontal gap opening.

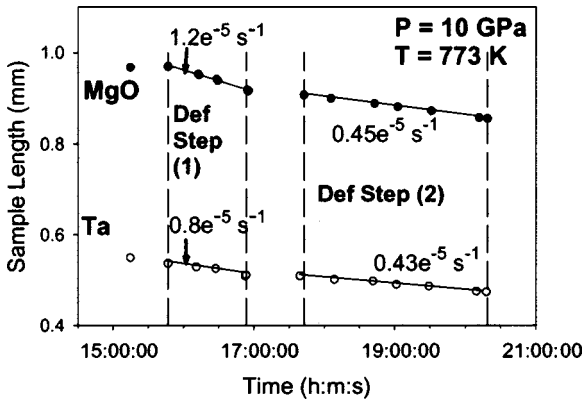

FIG. 10. Total axial length change of the two polycrystalline samples (MgO and Ta) deformed at 10 GPa and 773 K. Note the samples deform at different rates, especially during the first deformation step (1.2 vs 0.8 $\times10^{-5}$ s^{-1} for MgO and Ta, respectively), after which, the MgO sample shortened more substantially while the differential piston advancement was stopped (the waiting period between the two deformation steps). During the second deformation step, the strain rate of MgO is only slightly faster than that of Ta.

after 23.4% axial shortening. In this figure, Debye rings are converted into straight lines for ease of visualization. A monochromatic beam at 50 keV was used, corresponding to a wavelength of 0.248 Å. The vertical axes are azimuth angles, from 0° to 360° (from bottom to top), of the Debye rings, with 0° arbitrarily defined as diffraction vector being horizontal (parallel to the minimum principal stress axis), and the horizontal axes are 2θ, from 0° to 10° (left to right). Distortion in the Debye rings is clearly visible at 9 GPa, especially for the strong peak (200). The sinusoidal shape of

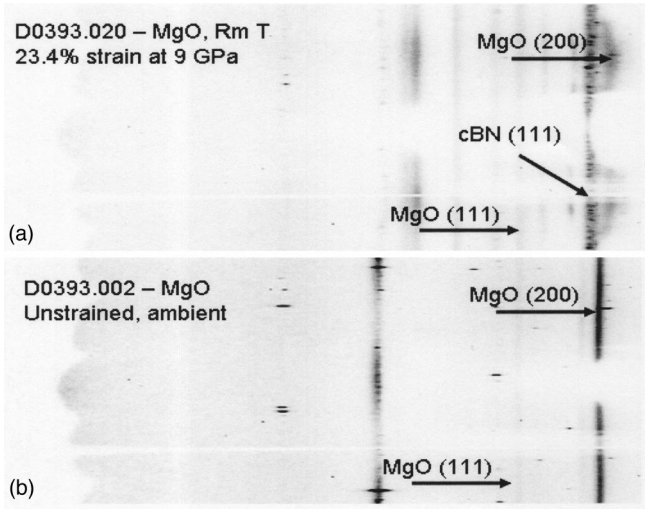

FIG. 11. Comparison of diffraction lines of MgO under (A) ambient $P-T$ condition (stress free) and (B) at 9 GPa and room temperature, after 24% shortening. The Debye rings have been transformed into straight lines to allow easy recognition of the distortion. Horizontal axes are two-theta from 0° to about 10°, and vertical axes azimuth angle Ψ measured from 0° (horizontal and perpendicular to the shortening axis σ_1) to 360°. Certain intensity variations are due to the shadowing of the cBN anvils. Modulated distortion in the 111 and 200 lines in MgO are evident. Due to the lack of collimation, diffractions lines from the surrounding materials are also present at high pressure (when the anvils gaps are small), with the cBN 111 line being the most prominent, the rest being from graphite (heater) and hexagonal BN (liner).

the 200 line has maxima in 2θ, which correspond to minima in d_{200}, near azimuths of 90° and 270°, which are parallel to the direction of the shortening. Likewise, the minima in 2θ at azimuths of 0° and 180° correspond to the minimum principle stress direction (horizontal).

Analysis of the effect of a uniaxial stress field for anisotropic crystals has been discussed by several authors.[32,33] The response of any d spacing (hkl) in a polycrystalline sample with random grain orientation to an axisymmetric differential stress field $(\sigma_1, \sigma_2 = \sigma_3)$ is given by

$$d_m(hkl) = d_P(hkl)[1 + (1 - 3\cos^2\Psi) \times (\sigma_1 - \sigma_3)Q(hkl)],$$

where $d_m(hkl)$ is the measured d spacing under pressure and stress, $d_P(hkl)$ the d spacing under hydrostatic pressure without influence of differential stress, Ψ the azimuth angle (measured from maximum principle stress direction), and $Q(hkl)$ an effective elastic compliance related to the specific crystallographic orientation of the lattice plane (hkl). Thus, with sufficient knowledge of elastic constants and their pressure and temperature dependence, differential stress can be extracted from lattice strain, if the material exhibits an elasto–plastic behavior.

Although stress measurements are based on elastic distortion in a crystalline lattice, it does not necessarily mean that we have to invoke an elasto–plastic model in measuring stress–strain curves for a given sample. As the sample of interest can be stacked with other ''reference'' materials in the deformation column, one can carefully select a ''piezometer,'' which, in an ideal situation, ought be inside the elastic region when the sample deforms nonelastically. The stress information obtained from the ''piezometer'' can then be used to infer the stress level in the sample. Two-dimensional monochromatic diffraction data are ideal in obtaining small distortions in the Debye rings. With a precision of 10^{-4} for the lattice spacing and a typical Young's modulus of 200 GPa it should be possible to resolve differential stresses of 20 MPa.

C. Other modes of experimentation

Once the cubic symmetry of the hydrostatic DIA is relaxed to tetragonal in the D-DIA and the coupling between hydrostatic pressure and deformation is removed, there are many ways to perform deformation experiments. One variation is to perform extension experiments under pressure as well as compression. We have carried out such experiments following compression tests by reversing motion on the differential and main rams. Pressure–time paths in the two modes are not precisely mirrored because of large hystereses in the overall mechanical system. In principle, such extension–compression cycles can be repeated in a single run. It has been demonstrated that pressure can be maintained in the hydrostatic DIA despite repeated reverse motion on the pyrophyllite gaskets.[31]

Another mode is to use anvils of different shapes to optimize gasket performance. With ordinary 45°-cut tungsten carbide anvils, the eight end-anvil gaskets will be under significant compression (pure shear) during deformation. Sample loading efficiency is poor in this circumstance because the gaskets must be continuously thinned. With end (upper and lower) anvils having an angle cut at 26.6° [$=\arctan(0.5)$], volume-compensating motion of end and side anvils is such that end-anvil gaskets have a constant thickness as the end anvils advance. Loading efficiency is improved, and larger deformations are possible. We have carried out preliminary measurements with 26.6°-cut anvils and verified that pressure efficiency is indeed better and larger deformations are feasible. However, total force (and therefore pressure) is limited by the higher shear stresses that are generated in the narrower end anvils, due to the lack of lateral support provided by the gaskets.

ACKNOWLEDGMENTS

The authors thank P. Murry, C. Pullin, and P. Dell for technical discussions and drafting of the original design of the D-DIA; D. Ruddle, C. Koleda, M. Jagger, and G. Hermannsdoerfer for setting up the D-DIA for our experiments; and T. Uchida, S. Mei, D. Frost, J. Chen, M. Vaughan, L. Li, and P. Burnley for contributions in carrying out some of the experiments. Work performed under the auspices of the U.S. Department of Energy by the Lawrence Livermore National Laboratory under Contract No. W-7405-ENG-48. Portions of this work were performed at GeoSoilEnviroCARS (GSECARS), Sector 13, Advanced Photon Source at Argonne National Laboratory. They authors also thank Mark Rivers, Steve Sutton, and GSECARS personnel for their support during the design and testing of the D-DIA. GSECARS is supported by the National Science Foundation-Earth Sciences, Department of Energy-Geosciences, W. M. Keck Foundation, and the U.S. Department of Agriculture. Use of the Advanced Photon Source was supported by the U.S. Department of Energy, Basic Energy Sciences, Office of Energy Research, under Contract No. W-31-109-Eng-38.

[1] M. S. Paterson, in *The Brittle-Ductile Transition in Rocks*, edited by A. G. Duba *et al.* (AGU, Washington, DC, 1990), pp. 187–194.
[2] R. S. Borch and H. W. Green, II, Nature (London) **330**, 345 (1989).
[3] Q. Bai and H. W. Green, II, in *Properties of Earth and Planetary Materials, Geophysical Monograph 101*, edited by M. Manghnani and T. Yagi (AGU, Washington, D.C., 1998), pp. 461–472.
[4] J. Renner, B. Stoeckhert, A. Zerbian, K. Roeller, and F. Rummel, J. Geophys. Res. **106**, 19411 (2001).
[5] R. Jeanloz, Phys. Today **53**, 44 (2000).
[6] P. W. Bridgman, J. Appl. Phys. **24**, 560 (1953).
[7] G. L. Kinsland and W. A. Bassett, J. Appl. Phys. **48**, 978 (1975).
[8] C. M. Sung, C. Goetze, and H. K. Mao, Rev. Sci. Instrum. **48**, 1386 (1977).
[9] C. Meade and R. Jeanloz, J. Geophys. Res. **93**, 3270 (1988).
[10] C. Meade and R. Jeanloz, J. Geophys. Res. B **93**, 3261 (1988).
[11] C. Meade and R. Jeanloz, Nature (London) **348**, 533 (1990).
[12] M. Chai, J. M. Brown, and Y. Wang, in *Earth and Planetary Materials at High Pressure and Temperature, Geophysical Monograph 56*, edited by M. Manghnani and T. Yagi (AGU, Washington, D.C., 1998), pp. 483–493.
[13] A. Fujimura, in *Rheology of Solids and of the Earth*, edited by S. Karato and M. Toriumi (Oxford University Press, Oxford, 1989), pp. 263–283.
[14] H. W. Green II, T. E. Young, D. Walker, and C. H. Scholz, in *High-Pressure Research: Application to Earth and Planetary Sciences*, edited by Y. Syono and M. H. Manghnani (Terra Scientific, Tokyo, 1992), pp. 229–235.
[15] H. W. Green, II, T. E. Young, D. Walker, and C. H. Scholz, EOS Trans. Am. Geophys. Union **71**, 1567 (1990).
[16] G. Y. Bussod, T. Katsura, and D. C. Rubie, PAGEOPH **141**, 579 (1993).

[17] S. Karato and D. C. Rubie, J. Geophys. Res. **102**, 20111 (1997).
[18] W. B. Durham and D. C. Rubie, in *Earth and Planetary Materials at High Pressure and Temperature, Geophysical Monograph 56*, edited by M. Manghnani and T. Yagi (AGU, Washington, D.C., 1998), pp. 63–70.
[19] S. Karato, C. Dupas-Bruzek, and D. C. Rubie, Nature (London) **395**, 266 (1998).
[20] P. Cordier and D. C. Rubie, Mater. Sci. Eng., A **309–310**, 38 (2001).
[21] D. Yamazaki and S. Karato, Rev. Sci. Instrum. **72**, 4207 (2001).
[22] N. L. Carter, J. M. Christie, and D. T. Griggs, J. Geol. **72**, 687 (1964).
[23] M. Shimada, Tectonophysics **72**, 343 (1981).
[24] J. Osugi, K. Shimizu, K. Inoue, and K. Yasunami, Rev. Phys. Chem. Jpn. **34**, 1 (1964).
[25] O. Shimomura, S. Yamaoka, T. Yagi, M. Wakatsuki, K. Tsuji, H. Kawamura, N. Hamaya, O. Fukuoga, K. Aoki, and S. Akimoto, in *Solid State Physics Under Pressure*, edited by S. Minomura (Terra Scientific, Tokyo, Japan, 1985), pp. 351–356.
[26] K. Inoue and T. Asada, Jpn. J. Appl. Phys. **12**, 1786 (1973).
[27] D. J. Weidner, M. T. Vaughan, J. Ko, Y. Wang, X. Liu, A. Yeganeh-Haeri, R. E. Pacalo, and Y. Zhao, in: *High-Pressure Research: Application to Earth and Planetary Sciences*, edited by Y. Syono and M. H. Manghnani (Terra Scientific, Tokyo, 1992), pp. 13–17.
[28] Y. Wang, M. Rivers, T. Uchida, P. Murray, G. Shen, S. Sutton, J. Chen, Y. Xu, and D. Weidner, in *Proceedings of the International Conference on High Pressure Science and Technology (AIRAPT-17)*, Honolulu, Hawaii, 25–30 July 1999 (University Press (India) Ltd., Hyderabad, India, 2000), pp. 1047–1052.
[29] O. Shimomura, W. Utsumi, T. Taniguci, T. Kikegawa, and T. Nagashima, in *High-Pressure Research: Application to Earth and Planetary Sciences*, edited by Y. Syono and M. H. Manghnani (Terra Scientific/American Geophysical Union, Washington, DC, 1992), pp. 3–11.
[30] W. Utsumi, T. Yagi, K. Leinenweber, O. Shimomura, and T. Taniguchi, in *High-Pressure Research: Application to Earth and Planetary Sciences*, edited by Y. Syono and M. H. Manghnani (Terra Scientific/American Geophysical Union, Washington, DC, 1992), pp. 37–42.
[31] Y. Wang, I. C. Getting, D. J. Weidner, and M. T. Vaughan, in *Properties of Earth and Planetary Materials, Geophysical Monograph 101*, edited by M. Manghnani and T. Yagi (AGU, Washington, D.C., 1998), pp. 35–39.
[32] A. K. Singh, J. Appl. Phys. **73**, 4278 (1993).
[33] T. Uchida, N. Funamori, and T. Yagi, J. Appl. Phys. **80**, 739 (1996).
[34] M. L. Rivers, T. S. Duffy, Y. Wang, P. J. Eng, and S. R. Sutton, in *Properties of Earth and Planetary Materials at High Pressure and Temperature*, edited by M. H. Manghnani and T. Yagi (American Geophysical Union, Washington, DC, 1998), pp. 79–88.
[35] H. A. Canistraro, E. H. Jordan, and D. M. Pease, Rev. Sci. Instrum. **69**, 452 (1998).
[36] W. Utsumi, D. J. Weidner, and R. C. Liebermann, in *Properties of Earth and Planetary Materials, Geophysical Monograph 101*, edited by M. Manghnani and T. Yagi (AGU, Washington, D.C., 1998), pp. 327–333.
[37] L. Bragg, Nature (London) **149**, 511 (1942).
[38] A. R. Stokes, K. J. Pascoe, and H. Lipson, Nature (London) **151**, 137 (1943).
[39] G. B. Greenough, in *Progress in Metal Physics*, edited by I. Chalmers (Interscience, New York, 1952), Vol. 3, pp. 176–219.
[40] D. J. Weidner, in *Reviews in Mineralogy*, edited by P. H. Ribbe (Mineralogical Society of America, Washington, D.C., 1998), pp. 493–524.